ОПТИКА И СПЕКТРОСКОПИЯ, 2003, том 94, № 5, с. 807–814

НЕКЛАССИЧЕСКИЕ СОСТОЯНИЯ СВЕТА

УДК 535.14

RATE-EQUATION APPROACH TO LASER LIGHT STATISTICS

© 2003 г. L. Chusseau*, J. Arnaud**, and F. Philippe***

* Centre d'É lectronique et de Micro-optoélectronique de Montpellier, UMR 5507 CNRS, Université Montpellier II, Montpellier, F34095 France

E-mail: chusseau@univ-montp2.fr

** Mas Liron, Saint Martial, F30440 France

E-mail: arnaudj2@wanadoo.fr

*** Laboratoire d'Informatique de Robotique et de Microélectronique de Montpellier, UMR 5506 CNRS, Montpellier, F34392 France

E-mail: Fabrice.Philippe@univ-montp3.fr

Поступила в редакцию 25.11.2002 г.

Single-mode cavity laser light statistics is considered within the framework of rate-equations. According to that approach, fluctuations are caused by jumps in active and detecting atoms. The algebra is simple allowing analytical expressions for intra-cavity Fano factor and photo-current spectral density to be obtained. Poissonian, quiet, and optical pumps are considered. The results are verified by comparison with Monte-Carlo simulations. An essentially exhaustive investigation of sub-Poissonian light generation by classical laser schemes, two-mode lasers and semiconductor lasers is proposed.

Неклассические состояния света и статистика нелинейно-оптических взаимодействий

INTRODUCTION

Light is called sub-Poissonian when the variance of the number of photo-detection events counted over a large time duration is less than the average number of events. Equivalently, we may say that the photo-current spectral density is below the shot-noise level at low Fourier (or baseband) frequencies. It has been shown experimentally by Machida *et al.* [1] that laser diodes driven by high-resistance electrical sources may generate sub-Poissonian light. This feature of great fundamental and practical importance treated theoretically by Golubev and Sokolov [2], Yamamoto *et al.* [3] on the basis of the laws of Quantum Optics may be understood alternatively as resulting from a birth-death Markov process efficiently modelled using Langevin forces and rate-equations (see Arnaud [4, 5] for an introduction to the method).

The purpose of this paper is to apply the rate-equation approach to various laser schemes, namely optically pumped 3- and 4-level lasers, two-mode lasers and electrically pumped semiconductor lasers. The light statistics is calculated either analytically or using Monte-Carlo techniques. The analytical expressions obtained from rate-equations are found to coincide with those derived from Quantum Optics methods, but the algebra is considerably simpler. This is so even when the emitted light exhibits sub-Poissonian statistics. To wit, the expression for the internal cavity statistics of many 4-level atoms with a negligible spontaneous decay previously given by Ritsch *et al.* [6] is recovered [7]. Similarly, 3-levels atoms expressions obtained by Khazanov *et al.* [8] are recovered (see below). Coherently-pumped 3-level atoms lasers [7] and two-mode lasers were apparently not treated earlier.

Rate-equations treat the number of photons in the cavity as a classical random function of time. The light field is quantized as a result of matter quantization and conservation of energy, but not directly. Rate equations should be distinguished from semi-classical theories in which the optical field is driven by atomic dipole expectation values. The theory employed in this paper rests instead on the consideration of transition probabilities, as in the Loudon [9] treatment of optical amplifier noise, for example. Every absorption event reacts on the number of light quanta in the optical cavity. Semi-classical theories are unable to explain sub-Poissonian light statistics because the light generation process and the light detection process are considered separately. We treat here the laser as a birth-death Markov process [10]. A Monte-Carlo simulation gives the evolution of the number m of photons in the cavity from which the Fano factor $\mathcal{F} = \mathrm{var}(m)/\langle m\rangle$ is obtained [7]. On the other hand, the instants t_k when photons are being absorbed provide the spectral density of the photo-current whose normalized value $\mathcal{S}$ is unity for Poisson processes [11]. The normalized spectrum is denoted $\mathcal{S}(\Omega)$. The Fourier angular frequency Ω is called for short: "frequency". When both the number of atoms and the pumping level increase, the computing time becomes prohibitively large because of the exponentially growing number of events to process. For simple laser schemes, analytical

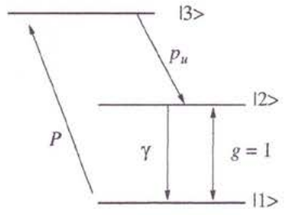

Fig. 1. V–type 3-level laser under incoherent (unidirectional) optical pumping.

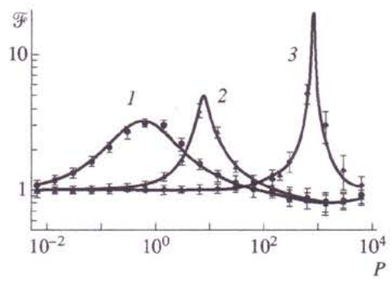

Fig. 2. Intra-cavity Fano factor for V–type lasers as a function of the pumping rate P. Error bars are the 95% confidence level from a statistical treatment applied to ten Monte-Carlo runs, each having duration $T_m = 200$. Plain lines are analytical. The parameters are: $N = 100$, $p_u = 632$, $\alpha = 6.32$, $\gamma = 0$ (*1*), 6.32 (*2*), 632 (*3*).

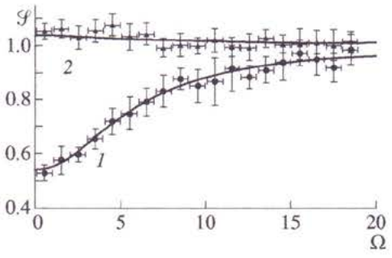

Fig. 3. Normalized photo-current spectral density $\mathcal{S}$ of V–type lasers as a function of Fourier frequency Ω. Points with error bars are from Monte-Carlo simulations with 150 runs, each of duration $T_m = 100$. Plain lines are analytical. The parameters are: $N = 100$, $p_u = 632$, $\alpha = 6.32$; *1* – $\gamma = 0$, $P = 1265$; *2* – $\gamma = 6.32$, $P = 20$.

expressions are obtained by applying the weak-noise approximation.

In Sec. II the rate-equation method is applied to V–type 3-level lasers using both Monte-Carlo simulations and the weak-noise approximation. The numerical method and the analytical method are found to agree for the range of parameters considered. More extensive treatments considering other laser schemes will appear elsewhere [7, 12]. Sec. III describes the complete treatment of a two-mode laser derived from a classical 4-level scheme. Well-known experimental results relative to partition noise will be shown to follow from the coupled rate equations. Semiconductor lasers are treated in Sec. IV. The Monte-Carlo simulation exhibits the combined influences of carrier heating and spectral hole burning on the dynamics of laser noise.

II. V–TYPE 3-LEVEL LASER

The active medium of V–type 3-level lasers is a collection of N identical atoms as depicted in Fig. 29. Level separations are supposed to be large compared with $k_B T$, where T denotes the optical cavity temperature and k_B the Boltzmann constant, so that thermally-induced transitions are negligible.

The probability per unit time that an electronic transition from level $|1\rangle$ to level $|2\rangle$ occurs is taken as equal to m, and the probability of an electronic transition from $|2\rangle$ to $|1\rangle$ as $m + 1$, where m denotes the number of photons in the cavity. This amounts to selecting a time unit whose typical value depends on the medium gain. Spontaneous decay from level $|2\rangle$ to level $|1\rangle$ is allowed with probability γ. This decay may be either non-radiative or involve radiation into other electromagnetic modes, besides the one of interest.

Photons are absorbed with probability αm, where α denotes a constant, the absorbing atoms residing most of the time in their ground state. These absorbing atoms model the transmission of light through mirrors with subsequent absorption by a detector. Provided detection is linear and reflectionless, it is immaterial whether absorption occurs inside or outside the optical cavity. Like in the Sargent *et al.* [13] classical textbook, it is convenient to consider absorbing atoms located inside the cavity. For simplicity, internal absorption is neglected.

"Incoherent" pumping promotes electrons from level $|1\rangle$ to level $|3\rangle$ with probability P. The case of "coherent" pumping that allows a fully symmetric electron exchange between levels $|1\rangle$ and $|3\rangle$ is discussed elsewhere [7]. When the pumping field originates from frequency-filtered thermal radiation, the pump fluctuations are nearly Poissonian.

Spontaneous decay from level $|3\rangle$ to the upper working level $|2\rangle$ occurs with probability p_u. All previously discussed relevant probabilities are schematized in Fig. 1.

A. Monte-Carlo Model

The rate-equation model of a N–atoms single-mode laser straightforwardly leads to a master equation for the probability of having m photons stored in the cavity at time t [5, 9, 14]. Alternatively, the laser evolution is modeled as a temporally homogeneous birth-death Markov process. In the steady-sate regime, rate of change and equilibrium probabilities of having m and $m + 1$ photons within the cavity are linked via detailed balancing condition. This is a favorable condition for a Monte-Carlo simulation [15] because every laser microstate belongs to a Markov chain and thus occurs proportionally to its equilibrium probability when the number of step increases to infinity.

For V–type 3-level lasers, rates of change W_j are ascribed to the different kinds of events as given in Table.

For example, the probability that an atom jumps from level $|1\rangle$ to level $|3\rangle$ during the elementary time interval $[t, t + \delta t]$ is $W_2 \delta t$, where δt is chosen small enough that this probability be much less than unity. Because atoms are coupled to one another only through the field, W_2 is proportional to the number n_1 of atoms in $|1\rangle$ at time t, and thus $W_2 = P n_1$, where the constant P is proportional to the pump strength. If a jump does occur, n_1 is reduced by 1 while the number n_3 of atoms in level $|3\rangle$ is incremented by 1. If the initial value of n_3 is N the event does not occur. Similar observations apply to the other jump probabilities. Notice that the coherent emission rate W_3 is proportional to $m + 1$, following the Einstein prescription. This ensures that laser emission re-starts if extinction occurs. A key feature that distinguishes the present formulation from other rate-equation methods is that absorption of photons by the detector is included in the system description. Because detection is supposed to be linear, such events are taken to occur with a rate $W_1 = \alpha m$, where α expresses detector absorption.

An efficient algorithm has actually been employed [10]. Given that an event of any kind occurred at time τ_k, the next-event time is

$$\tau_{k+1} = \tau_k + \frac{1}{\sum_j W_j} \ln\left(\frac{1}{\mathrm{r}}\right), \qquad (1)$$

where r is a random number uniformly distributed in the interval [0, 1]. The probability that the event is of kind l is equal to $W_l / \sum_j W_j$. The Monte-Carlo method is readily implemented, only the total number of atoms in each state needs to be tracked (for fermions the numerical procedure is significantly more involved [11]). Within the whole time set $\{\tau_k\}$, we select the subset $\{t_k\}$ of photon-absorption events. It is then straightforward to evaluate the photo-detection noise spectrum.

The intra-cavity Fano factor $\mathcal{F}$ is represented in Fig. 2. The analytical results of Sec.6 agree well with the simulation. Notice that $\mathcal{F}$ is below unity within some pumping range. This behavior is in good agreement with previous Quantum-Optics results [6, 8, 16, 17].

The normalized spectral density $\mathcal{S}(\Omega)$ is represented in Fig. 3 for two sets of parameter values. For each Monte-Carlo run, $\mathcal{S}(\Omega)$ is first evaluated from the $\{t_k\}$ list [11] and refined using a smoother power spectral density estimator [18, 19]. Averaging over runs and concatenating neighboring frequencies produce the final data together with error bars at the 95% confidence level. There is fair agreement between Monte-Carlo simulations and analytical formulas to be subsequently reported. Both predict sub-Poissonian photo-current statistics. Even with one billion photon-absorption

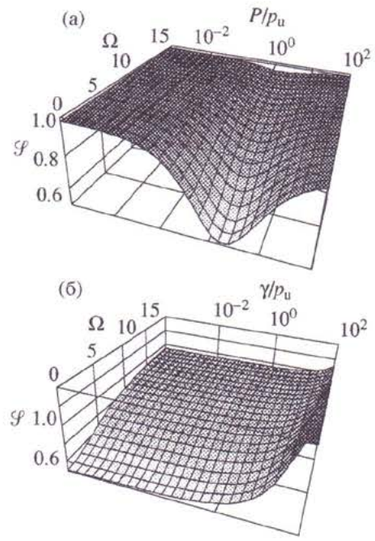

Fig. 4. 3D plot of $\mathcal{S}$ of a V–type laser as a function of Fourier frequency Ω and (a) normalized pumping rate P/p_u, (b) normalized recombination rate γ/p_u. The laser parameters are $N = 10^5$, $\alpha = 6.32$, $p_u = 632$. The more sub-Poissonian the light statistics, the lighter the surface.

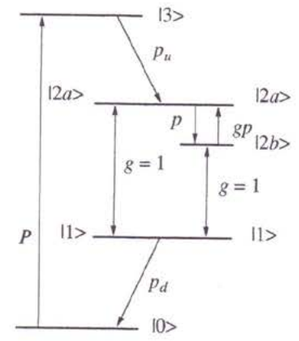

Fig. 5. Two-mode laser scheme.

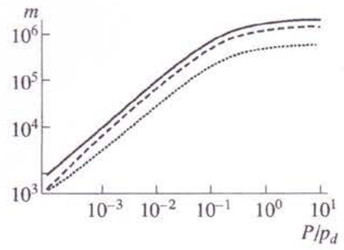

Fig. 6. Average number of photons in the cavity as a function of the normalized pumping level P/p_d. Dotted line: m_b, transition $|2b\rangle \longrightarrow |1\rangle$, dashed line: m_a, transition $|2a\rangle \longrightarrow |1\rangle$, Solid line: $m = m_a + m_b$, total of both transitions. Laser parameters are $N = 10^5$ atoms, $p_d = 632$, $p_u = 316$, $\alpha = 6.32$, $p = 1265$, $T = 300$ K.

events, Monte-Carlo spectra exhibit large error bars. An analytical method is to be preferred when it exists. On the other hand, Monte-Carlo simulations do not rely on linearization and provide a useful check.

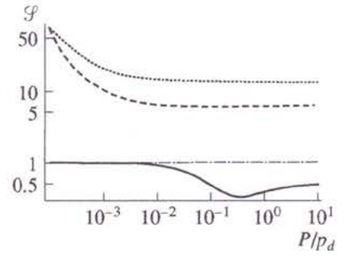

Fig. 7. Normalized spectral density, $\mathcal{S}$, of the two-mode laser. Line symbols and laser parameters are the same as in Fig. 6 except for the dot-dashed line that materializes the shot-noise level.

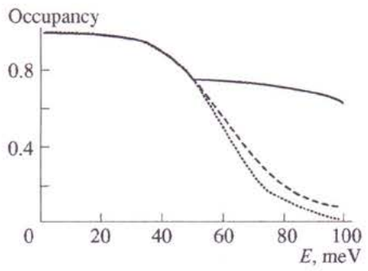

Fig. 9. Monte-Carlo electron occupancy in CB as a function of energy position E (referred to the CB bottom) and thermalization rate p. Lasing level is $E = 50$ meV. Dots: $p = 25000$ ns^{-1}, dashed line: $p = 1000$ ns^{-1}, solid line: $p = 250$ ns^{-1}.

B. Analytic Model

Let us first set up the steady-state conditions. If n_j, $j = 1, 2, 3$, denote the number of atoms in state j, we have

$$n_1 + n_2 + n_3 = N. \tag{2}$$

Let $\mathcal{J}$ denotes the net pumping rate, $\mathcal{R}$ the net stimulated rate, $\mathcal{U}$ the upper decay rate, $\mathcal{S}$ the spontaneous decay rate from the upper to the lower working levels, and $\mathcal{Q}$ the photon absorption rate. The steady-state conditions then read (8)

$$\mathcal{J} = \mathcal{U} = \mathcal{D} = \mathcal{R} + \mathcal{S}, \tag{3a}$$

$$\mathcal{Q} = \mathcal{R}, \tag{3b}$$

where

$$\mathcal{J} = Pn_1, \quad \mathcal{U} = p_u n_3, \tag{4a}$$

$$\mathcal{S} = \gamma n_2, \quad \mathcal{Q} = \alpha m, \tag{4b}$$

$$\mathcal{R} = (m+1)n_2 - mn_1. \tag{4c}$$

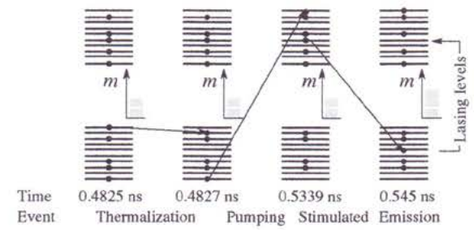

Fig. 8. Four-frame sequence illustrating the Monte-Carlo simulation of a semiconductor laser. 10 equally-spaced energy levels are considered in VB and CB. Insets represents the number of photon m stored in the cavity at some time by stacked bricks. Arrows show electron moves from one energy level to another.

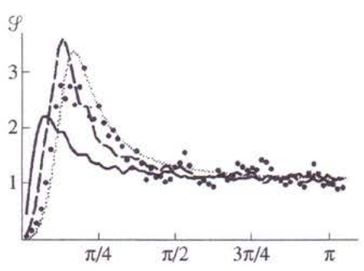

Fig. 10. Monte-Carlo normalized spectral density $\mathcal{S}$ as a function of normalized Fourier angular pulsation Ω. Gray curve is the analytical calculation assuming perfect thermalization from Eq. (22). Dots: $p = 25000$ ns^{-1}, dashed line: $p = 1000$ ns^{-1}, solid line $p = 250$ ns^{-1}.

A straightforward solution of Eqs. (2), (3) and (4) provides the steady-state atomic populations n_i and photon number m.

Within the weak-noise approximation, populations and rates are split into steady-state values and fluctuations. The instantaneous photon number m is thus written as $\langle m \rangle + \Delta m$, where $\langle m \rangle$ denotes the steady-state value. For rates, fluctuations consist of a deterministic function and uncorrelated Langevin "forces", i.e., $J = \langle \mathcal{J} \rangle + \Delta J$, the ΔJ term including a Langevin force $j(t)$ expressing the jump process randomness. Thus

$$\mathcal{J} \equiv J + \Delta J, \quad \mathcal{U} \equiv U + \Delta U, \tag{5a}$$

$$\mathcal{S} \equiv S + \Delta S, \quad \mathcal{Q} \equiv Q + \Delta Q, \tag{5b}$$

$$\mathcal{R} \equiv R + \Delta R, \tag{5c}$$

where a first-order variation of the expressions in Eq. (4) yields

$$\Delta J = P\Delta n_1 + j, \tag{6a}$$

$$\Delta R = (m+1)\Delta n_2 - m\Delta n_1 + (n_2 - n_1)\Delta m + r, \tag{6b}$$

$$\Delta S = \gamma \Delta n_2 + s, \tag{6c}$$

$$\Delta U = p_u \Delta n_3 + u, \tag{6d}$$

$$\Delta Q = \alpha \Delta m + q. \tag{6e}$$

Similarly, a first-order variation of the population conservation rule gives

$$0 = \Delta n_1 + \Delta n_2 + \Delta n_3. \tag{7}$$

Let us consider first zero-frequency noise. Eq. 3, when applied to variations, reads

$$\Delta J = \Delta U = \Delta R + \Delta S, \tag{8a}$$

$$\Delta Q = \Delta R. \tag{8b}$$

Replacing atomic populations and photon numbers by their steady-state values, the above set of equations has been solved. In particular, ΔQ is obtained as a linear combination of the Langevin forces

$$\Delta Q = \sum_{z \in \{j,u,q,r,s\}} c_z z, \tag{9}$$

where the c_z are real coefficients that depend on the parameters N, P, p_u, γ and α. The detailed expressions, too lengthy to be given here in their general form, are conveniently handled using symbolic calculations.

The normalized zero-frequency photo-current spectral density is of the form

$$\mathcal{F} = \frac{1}{\alpha m} \sum_{z \in \{j,u,q,r,s\}} c_z^2 \sigma_z, \tag{10}$$

where σ_z denotes the spectral density value of the Langevin noise source z, equal to average rates,

Elementary events in V-type 3-level lasers (see Fig. 1) and corresponding rate of change W_j

Event	Transition	Rate
photon absorption	–	$W_1 = \alpha m$
pump absorption	$\|1\rangle \longrightarrow \|3\rangle$	$W_2 = Pn_1$
coherent emission	$\|2\rangle \longrightarrow \|1\rangle$	$W_3 = (m+1)n_2$
coherent absorption	$\|1\rangle \longrightarrow \|2\rangle$	$W_4 = mn_1$
spotaneous decay	$\|2\rangle \longrightarrow \|1\rangle$	$W_5 = \gamma n_2$
upper decay	$\|3\rangle \longrightarrow \|2\rangle$	$W_6 = n_3 p_u$

$$\sigma_j = Pn_1, \quad \sigma_u = p_u n_3, \tag{11a}$$

$$\sigma_s = \gamma n_2, \quad \sigma_q = \alpha m, \tag{11b}$$

$$\sigma_r = (m+1)n_2 + mn_1. \tag{11c}$$

When these expressions are introduced in Eq. (10) an analytical expression of $\mathcal{F}$ is obtained.

Consider now the very special case where $\gamma = 0$ and $N \gg \alpha$, i.e., the laser is thresholdless and has very low loss. The normalized photo-current spectral density reads

$$\mathcal{F} = 1 - \frac{4Pp_u}{(P + 2p_u)^2}. \tag{12}$$

$\mathcal{F}$ is thus unity at low and high pumping levels and goes to a minimum in between these bounds. The minimum value, $\mathcal{F}_{\min}$, and the corresponding pumping value are

$$\mathcal{F}_{\min} = \frac{1}{2}, \quad P = 2p_u. \tag{13}$$

It can be shown that this minimum is the absolute minimum of $\mathcal{F}$, irrespectively of the values of γ, N and α [7].

A similar technique applied to Λ–type 3-level laser and 4-level laser leads to $\mathcal{F}_{\min} = 1/2$ and $\mathcal{F}_{\min} = 1/3$, respectively. These values are in complete agreement with 3-levels theories proposed earlier by Khazanov *et al.* [8] and by ralph:PRA91,ralph:QO93 and with the 4-level theory by Ritsch *et al.* [6].

At some Fourier frequency Ω the generalized rate equations read [4]

$$i\Omega \Delta m = \Delta R - \Delta Q, \tag{14a}$$

$$i\Omega \Delta n_1 = \Delta R + \Delta S - \Delta J, \tag{14b}$$

$$i\Omega \Delta n_2 = \Delta U - \Delta R - \Delta S, \tag{14c}$$

$$i\Omega \Delta n_3 = \Delta J - \Delta U. \tag{14d}$$

Again, we solve for ΔQ the linear system of fluctuations and obtain for the normalized spectral density

$$\mathcal{F}(\Omega) = \frac{1}{\alpha m} \sum_{z \in \{j,u,q,r,s\}} \tilde{c}_z(\Omega) \hat{c}_z^*(\Omega) \sigma_z, \tag{15}$$

where the coefficients $\tilde{c}_z$ are complex and frequency dependent and where the Langevin "forces" σ_z are still given in Eq. (11).

After rearranging, Eq. (15) gives the spectral density in the form

$$\mathcal{J}(\Omega) = 1 + \frac{a_2\Omega^4 + a_1\Omega^2 + a_0}{\Omega^6 + b_2\Omega^4 + b_1\Omega^2 + b_0}, \qquad (16)$$

where the coefficients a_i and b_i are real. The form in Eq. (16) ensures that $\mathcal{J}(\Omega)$ tends to shot-noise level at high frequencies. Fig. 4 shows that $\mathcal{J}(\Omega)$ reaches its minimum value at $\Omega = 0$.

When spontaneous decay from the upper working level may be neglected (Fig. 4 (a)), light is always sub-Poissonian and the lowest $\mathcal{J}$–value occurs when $P/p_u = 2$. Figure 4 (b) illustrates the fact that spontaneous decay from the upper working level is inconsequential until $\gamma/p_u \approx 3 \times 10^{-2}$. However, the light statistics ceases to be sub-Poissonian when $\gamma/p_u > 0.3$ because the lasing threshold can not be reached anymore.

The intra-cavity photon statistics is characterized by the Fano factor $\mathcal{F} = \langle\Delta m^2\rangle/\langle m\rangle$, where m denotes as before the number of photons in the cavity. The variance of m equals the integration over frequency of $\mathcal{J}_{\Delta m}(\Omega)$, the normalized spectral density of Δm. As previously, $\mathcal{J}_{\Delta m}(\Omega)$ obtains by solving for Δm instead of ΔQ and its general form is

$$\mathcal{J}_{\Delta m}(\Omega) = \frac{a_2'\Omega^4 + a_1'\Omega^2 + a_0'}{\Omega^6 + b_2'\Omega^4 + b_1'\Omega^2 + b_0'}, \qquad (17)$$

where a_i' and b_i' are real coefficients. The Fano factor is thus

$$\mathcal{F} = \int_{-\infty}^{\infty} \mathcal{J}_{\Delta m}(\Omega)\frac{d\Omega}{2\pi}. \qquad (18)$$

It has been already illustrated in Fig. 2 and successfully compared to Monte-Carlo calculations.

III. TWO-MODE LASER

Consider now a two-mode laser and let us focus on normalized spectral densities of each individual mode and of the total laser emission. As shown in Fig. 5, the scheme starts from the 4-level laser. The upper lasing level $|2\rangle$ has been split into two sub-levels $|2a\rangle$ and $|2b\rangle$, both being able to relax radiatively toward level $|1\rangle$. Optical gains of these two transitions are kept identical.

The beating between the two optical modes is arbitrarily prescribed at a 1 THz frequency. Corresponding energy splitting is thus $\varepsilon = 4.1$ meV. The coupling $|2a\rangle \longrightarrow |2b\rangle$ is ensured by a transfer parameter p. The coupling $|2b\rangle \longrightarrow |2a\rangle$ is slightly less, e.g. qp. As driven by temperature it refills level $|2a\rangle$ from $|2b\rangle$ according to Boltzmann law, $q = \exp(-\varepsilon/k_BT)$. Atomic populations are supposed to be unable to respond to the very high modal beat frequency.

It is straightforward to identify physical processes and corresponding rates by analogy with previous discussion of Sec. II. Let us moreover assume a weak coupling between the two modes just like in the sargent textbook. Thus both modes truly exist. For the sake of simplicity, non-radiative relaxations $|2a\rangle \longrightarrow |1\rangle$ and $|2b\rangle \longrightarrow |1\rangle$ are neglected and the photon count of each mode is supposed far greater than unity, $m_a \gg 1$ and $m_b \gg 1$. Rates thus read

$$\mathcal{P} = Pn_0, \quad \mathcal{U} = p_u n_3, \qquad (19a)$$

$$\mathcal{R}_a = m_a(n_{2a} - n_1), \quad \mathcal{T} = pn_{2a} - qpn_{2b}, \qquad (19b)$$

$$\mathcal{R}_b = m_b(n_{2b} - n_1), \quad \mathcal{D} = p_d n_1, \qquad (19c)$$

$$\mathcal{Q}_a = \alpha m_a, \quad \mathcal{Q}_b = \alpha m_b. \qquad (19d)$$

The stable two-mode steady-state solution is calculated using conservation rules for populations and rates. Of major interest are the modal steady-state photon numbers

$$m_b = \frac{(1-q)p(P(N+\alpha)p_u + \alpha p_d(P+p_u))}{\alpha(3Pp_u + p_d(P+p_u))}, \qquad (20a)$$

$$m_a = \frac{Pp_d(p_u(N-2\alpha) - \alpha p(1-q))}{\alpha(3Pp_u + p_d(P+p_u))} - m_b. \qquad (20b)$$

Figure 6 represents the average number of photons in the cavity for a particular choice of $p = 4p_u$ that roughly balances the two mode powers. Like for optically pumped single-mode lasers [7], m increases regularly with pump intensity and saturates at very high level because of ground-state population depletion.

As was done before in Sec.6, total rates and populations are split into average values and variations. We evaluate the normalized zero-frequency photo-current spectral densities for each mode and for the total laser output. The Fig. 7 gives plots of photodetection spectral densities of each mode and of the total emitted light. Again the parameter is the pumping P.

The total photodetection spectral density is nearly the same as for single-mode 4-level lasers. Here again, sub-Poissonian behavior is observed at high pumping levels [7]. It can be shown that when α tends to 0, $\mathcal{J}$ reduces to

$$\mathcal{J} = \frac{9P^2p_u^2 + p_d^2(P^2 + p_u^2)}{(3Pp_u + p_d(P+p_u))^2}, \qquad (21)$$

which admits the minimum value $\mathcal{J}_{\min} = 1/3$ if $P = p_u = p_d/3$. Although pumping conditions are slightly different, the $\mathcal{J}_{\min}$ value is the same as for usual 4-level lasers [6, 7].

The most important feature of Fig. 7 appears on individual mode spectral densities $\mathcal{J}_a$ and $\mathcal{J}_b$ that are much more 'noisy' than previous total spectral density $\mathcal{J}$. Moreover, any attempt to balance mode powers maximizes $\mathcal{J}_a$ and $\mathcal{J}_b$. This effect, usually referred to as the mode-partition noise, has often been observed. It is very easily and straightforwardly explained from the present rate-equation approach.

IV. SEMICONDUCTOR LASER

Actual semiconductor lasers are complex systems. An idealized model will prove helpful. One-electron energy levels in the semiconductor are supposed to be of the form $\epsilon_k = k\epsilon$, with k an integer and ε a constant, e.g. $\varepsilon = 1$ meV. Allowed levels may be occupied by at most one electron to comply with the Pauli exclusion principle. The electron spin, ignored in the present paper for the sake of brevity, is discussed for example in [21]. Our model considers neither electronic superposition states nor any strong Coulomb interaction, approximations made in virtually all laser-diode theories. In semiconductors the allowed electronic levels group into two bands, the conduction band (CB) and valence band (VB). We suppose that both bands involve the same number of levels. The band gap energy is instrumental in determining the laser oscillation frequency but it will not enter in our model because of simplifying assumptions to be later discussed. The number of electrons matches the number of allowed energy levels so that the electron-lattice system is electrically neutral. For pure semiconductors at $T = 0$ K, the N electrons fill up the valence band while the conduction band is empty.

Rate-equation approach first requires the identification of the elementary Markov processes that electrons and photons follow. Photon absorption is supposed to be only due to detecting atoms, that is, no additional optical loss is considered. Detecting atoms are assigned a probability αm of being promoted to the upper state, where α denotes a constant and m the number of photons in the cavity. Stimulated absorption occurs with a probability m for electrons in the lower working level to be promoted to the upper working level. Stimulated emission is modeled by assigning a probability $m + 1$ to electrons in the upper working level to be demoted to the lower working level. Setting as unity the factor that multiplies the expressions m or $m + 1$ amounts to selecting a time scale, e.g., 1 ns. In addition, the laser is assumed to be single-mode, and lasing is supposed to take place between levels located in the middle of CB and VB.

Only perfectly regular electrical pumping is considered. Since output photons reproduce (for slow variations) the electrical source statistics, the laser is expected to exhibit sub-Poissonian light statistics at low baseband frequencies [2]. Practical realizations involve the electrical current generated by a cold high-impedance electrical source, which is almost non-fluctuating as a consequence of the Nyquist theorem [3]. In the model, quiet electrical pumping is obtained by promoting low-lying electrons into high-lying levels periodically in time. As long as this time period remains short as compared to the time scales of interest, this prescription implies that the pumping rate is nearly constant.

Let us now consider the process of thermalization between the electron gas and the lattice. To enforce thermalization each electron is ascribed a probability p per unit time of being demoted to the adjacent lower level provided this level is empty, and a probability qp, where $q = \exp(-\varepsilon/k_BT)$ of being promoted to the adjacent upper level if it is empty. If p is large, thermalization is very efficient and electron-gas temperatures in both bands are equal to the lattice temperature. An analytic expression of the normalized spectral density can be obtained in that case [11, 22]

$$\mathcal{J}(\Omega) = 1 + \frac{\dfrac{\alpha(1+\alpha)}{1-\alpha}\dfrac{F}{J^*} - 1}{\dfrac{1-\alpha^2}{2\alpha^2}J^*F + (1-F)^2}, \qquad (22)$$

where, $F = \Omega^2/\Omega_r^2$, $\Omega_r^2 = (1-\alpha^2)J^*/2$, $J^* = (J\varepsilon)/(k_BT)$, J the pumping rate in electron per second, and α the cavity losses. To the contrary, if p is not large, electron gas temperatures are ill defined and the electronic populations are out of thermal equilibrium. Up to a point, a decrease of p is equivalent to an increase of the pumping rate.

The above description of semiconductor lasers permits Monte-Carlo calculation as depicted with the four successive frames given in Fig. 8. Three elementary processes are illustrated from a computer simulation involving only 10 levels in each bands. At the start, the system has already reached a stationary regime. A sample of the electron distribution is shown on the left. The corresponding time and the number of light quanta stored in the cavity are respectively $\tau_0 = 0.4825$ ns and $m = 2$. The first event at $\tau_1 = 0.4827$ ns is a VB thermalization. Its effect is to decrement the system energy by ε since an electron is demoted by one energy step. The second event at $\tau_2 = 0.5339$ ns is an electrical pumping event that promotes the VB electron occupying the lowest energy level to the highest energy level of the CB. The third event illustrates stimulated emission between the lasing levels at $\tau_3 = 0.545$ ns. As a result, the number of light quanta is incremented from $m = 2$ to $m = 3$.

Results of Monte-Carlo calculations are given in Figs. 9 and 10 where p, the rate at which thermalization events occur is taken as the main parameter of interest. The laser model includes 100 levels evenly-spaced by $\varepsilon = 1$ meV in each band. A lattice temperature of $T = 100$ K is assumed, thereby yielding $q \approx 0.89$. The regular pumping transfers one VB electron to CB at a rate of 5 ns^{-1}.

The occupancy in CB is plotted in Fig. 9 as a function of energy level E referred to the bottom of CB. As expected, a decrease of p (or an increase of pumping) modifies the CB occupancy. The Fermi-Dirac (FD) sta-

tistic is recovered at high p value, a regime where the analytical model of Eq. (22) is in good agreement with Monte-Carlo calculations. It is worth noting that sub-Poissonian light statistics is achieved at low baseband frequencies up to $\Omega \approx 0.1$.

At moderate p values, or equivalently at moderate pumping levels, the occupancy slightly departs from FD law and the frequency domain of sub-Poissonian light emission is reduced. A FD fit of the occupancy (dashed line in Fig. 9) gives a $T = 132$ K carrier temperature. Inserting this electron-gas revised temperature into Eq. (22) does not suffice to explain the Monte-Carlo results. In our opinion, spectral hole burning (SHB) may be responsible for the obtained spectrum, even though this effect does not appear conspicuously on the occupancy curves. As a secondary effect, the Ω–range over which light is sub-Poissonian get reduced by approximately fourty per cent.

At very high pumping rates, the SHB is conspicuous on the solid line of Fig. 9 and the Ω–range where sub-Poissonian light is observed gets reduced by approximately eighty per cent. The FD statistics evidently no more apply and $\mathcal{S}(\Omega)$ is no more described by Eq. (22). These Monte-Carlo results show that SHB and carrier thermalization are physical phenomena that one can not separate. Both act on the fluctuation spectra and the laser dynamics with the consequence of a reduction of the sub-Poissonian emission range.

V. CONCLUSION

The rate-equation approach was applied to various laser schemes. An accurate description of laser light statistics was obtained in every case, even when the laser light emission is sub-Poissonian because of a driving quiet pump or because of the depletion of the lower level by an intense optical pump.

For simple lasers schemes, fully analytical expressions were derived for the output light spectral density and the intracavity Fano factor. These expressions coincide with already published results available only for some laser schemes (3- and 4-level lasers) and special values of the parameters (no spontaneous recombination rate, infinitely low optical losses). On the other hand, the microscopic markovian approach underlying rate-equations was exploited in Monte-Carlo calculations. It was demonstrated to be fully equivalent to analytical calculations considering the V–type 3-level laser. A far more complicated laser scheme was considered in Monte-Carlo calculations, namely a quiet-pump semiconductor laser. The method offers new insights concerning the combined influence of carrier thermal heating and spectral hole burning that occur when pumping increases. Particularly, the reduction of the sub-Poissonian light emission range was demonstrated. Earlier work [23] has shown that the rate-equation method enables one to treat also phase fluctuations, excess noise, non-linear gain, multiphoton process, and electronic feedbacks from detectors to modulators.

ACKNOWLEDGMENTS

This work was supported by the STISS Department of Université Montpellier II and by CNRS under the JemSTIC Program.

FERERENCES

1. S. Machida, Y. Yamamoto, and Y. Itaya, Phys. Rev. Lett. 58, 1000 (1987).
2. Y. M. Golubev and I. V. Sokolov, Sov. Phys.-JETP 60, 234 (1984).
3. Y. Yamamoto, S. Machida, and O. Nilsson, Phys. Rev. A 34, 4025 (1986).
4. *J. Arnaud, Opt.* Quantum Electron. 27, 63 (1995).
5. *J. Arnaud, Opt.* Quantum Electron. pp. 393–410 (2002), quant-ph/0201151.
6. H. Ritsch, P. Zoller, C. W. Gardiner, and D. F. Walls, Phys. Rev. A 44, 3361 (1991).
7. L. Chusseau, J. Arnaud, and F. Philippe, Phys. Rev. A (2002), submitted, quant-ph/0203029.
8. A. M. Khazanov, G. A. Koganov, and E. O. Gordov, Phys. Rev. A 42, 3065 (1990).
9. R. Loudon, The Quantum Theory of Light (Oxford University Press, Oxford, 1983).
10. D. T. Gillespie, Markov Processes: An Introduction for Physical Scientists (Academic Press, San ?Diego, 1992).
11. L. Chusseau and J. Arnaud, Opt. Quantum Electron. (2002), to appear, quant-ph/0105078.
12. L. Chusseau, J. Arnaud, and F. Philippe, unpublished.
13. M. Sargent, III, M. O. Scully, and W. E. Lamb, Jr., Laser Physics (Addison-Wesley Publishing Company, Reading, MA, 1974).
14. M. O. Scully and W. E. Lamb, Jr., Phys. Rev. 159, 208 (1967).
15. D. P. Landau and K. Binder, A Guide to Monte Carlo Simulations in Statistical Physics (Cambrige University Press, Cambridge, 2000).
16. T. C. Ralph and C. M. Savage, Phys. Rev. A 44, 7809 (1991).
17. G. A. Koganov and R. Shuker, Phys. Rev. A 63, 015802 (2000).
18. A. Papoulis, Probability, Random Variables, and Stochastic Processes (Mac Graw-Hill, New York, 1991).
19. W. H. Press, S. A. Teukolsky, W. T. Vetterling, and B. P. Flannery, Numerical Recipes in C (Cambridge University Press, Cambridge, 1992).
20. T. C. Ralph and c. M. Savage, Quantum Opt. 5, 113 (1993).
21. J. Arnaud, L. Chusseau, and F. Phillippe, Phys. Rev. B 62, 13482 (2000).
22. J. Arnaud and M. Esteban, IEEE Proc. J. 137, 55 (1990).
23. *J. Arnaud, Electron.* Lett. 29, 1320 (1993).